ACS APPLIED MATERIALS & INTERFACES

Research Article

www.acsami.org

Controlled Delivery of Extracellular ROS Based on Hematoporphyrin-Incorporated Polyurethane Film for Enhanced Proliferation of Endothelial Cells

Min-Ah Koo,[∥,†,‡] Bong-Jin Kim,[∥,§] Mi Hee Lee,[†] Byeong-Ju Kwon,[†,‡] Min Sung Kim,[†,‡] Gyeung Mi Seon,[†,‡] Dohyun Kim,[†] Ki Chang Nam,[⊥] Kang-Kyun Wang,[§] Yong-Rok Kim,[*,§] and Jong-Chul Park[*,†,‡]

[†]Department of Medical Engineering and [‡]Brain Korea 21 PLUS Project for Medical Science, Yonsei University College of Medicine, 50-1 Yonsei-ro, Seodaemun-gu, Seoul 03722, Republic of Korea

[§]Department of Chemistry, Yonsei University, 50 Yonsei-ro, Seodaemun-gu, Seoul 03722, Republic of Korea

[⊥]Department of Medical Engineering, Dongguk University College of Medicine, Gyeonggi-do 10326, Republic of Korea

ABSTRACT: The principle of photodynamic treatment (PDT) involves the administration of photosensitizer (PS) at diseased tissues, followed by light irradiation to produce reactive oxygen species (ROS). In cells, a moderate increase in ROS plays an important role as signaling molecule to promote cell proliferation, whereas a severe increase of ROS causes cell damage. Previous studies have shown that low levels of ROS stimulate cell growth through PS drugs-treating PDT and nonthermal plasma treatment. However, these methods have side effects which are associated with low tissue selectivity and remaining of PS residues. To overcome such shortcomings, we designed hematoporphyrin-incorporated polyurethane (PU) film induced generation of extracellular ROS with singlet oxygen and free radicals. The film can easily control ROS production rate by regulating several parameters including light dose, PS dose. Also, its use facilitates targeted delivery of ROS to the specific lesion. Our study demonstrated that extracellular ROS could induce the formation of intracellular ROS. In vascular endothelial cells, a moderated increase in intracellular ROS also stimulated cell proliferation and cell cycle progression by accurate control of optimum levels of ROS with hematoporphyrin-incorporated polymer films. This modulation of cellular growth is expected to be an effective strategy for the design of next-generation PDT.

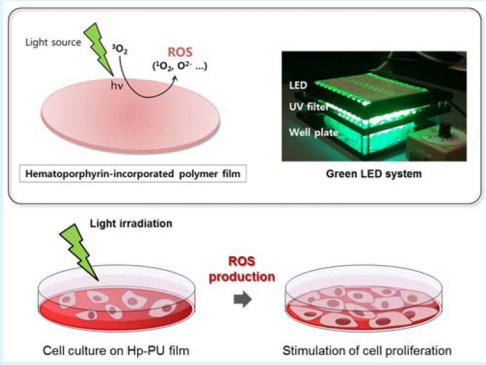

KEYWORDS: *photodynamic treatment, reactive oxygen species, Hp-PU film, localized delivery, endothelial cell proliferation*

1. INTRODUCTION

The term reactive oxygen species (ROS) broadly describes highly reactive ions or molecules including radical ROS such as superoxide anion (O_2^-), nitric oxide (NO), and hydroxyl radicals (OH·), as well as nonradical ROS such as hydrogen peroxide (H_2O_2), ozone (O_3), and singlet oxygen ($^1O_2$).[1−4] ROS play an essential role for biological functions. They act as signaling molecules to regulate many signal transduction pathways through reaction with and modification of the structure of proteins, transcription factors and genes to modulate various cellular functions.[2] A moderate increase in ROS can promote cell proliferation and differentiation, whereas excessive amounts of ROS can induce cell senescence and even cell death by causing oxidative damage to lipids, proteins, and DNA.[2,5−7] Recent studies suggested that low levels of ROS could be beneficial to cell growth and function. For example, Dandapat et al. showed that low concentrations of oxidized low-density lipoprotein induced generation of ROS and capillary tube formation in endothelial cells.[8] Blazquez-Castro et al. reported that photodynamic treatment with low concentrations of methyl 5-aminolevulinate promotes moderate production of endogenous ROS, that efficiently stimulates cell proliferation in human keratinocytes.[9]

Photodynamic treatment (PDT) is an efficient theranostic modality to utilize and generate ROS. The principle of PDT involves the systemic, local, or topical administration of a nontoxic drug or dye known as a photosensitizer (PS) followed by selective irradiation with light of an appropriate wavelength.[10,11] In the presence of oxygen, PS absorbs photons and is transformed from its ground state into an excited triplet state. It can react with cell membrane or a molecule, and transfer an electron to form radicals, which interact with oxygen to produce oxygenated products (type I reaction). On the other hand, the triplet can transfer its excitation energy directly to surrounding molecular oxygen, generating a highly ROS such as singlet oxygen (type II reaction). Both type I and type II reactions occur simultaneously, and the ratio between radical and nonradical ROS produced in these processes relies on the

Received: June 23, 2016
Accepted: October 4, 2016
Published: October 4, 2016

DOI: 10.1021/acsami.6b07628
ACS Appl. Mater. Interfaces 2016, 8, 28448−28457

type of PS used.[12−16] The primary aim of PDT is to treat selectively diseased tissues while having minimal impact on normal tissues. However, the current PDT, which systemically administers drugs or it-loaded nanocarriers, is often accompanied by severe systemic toxicity and long-term side effects in patients due to poor metabolic properties of PS and the lack of specificity for lesion. Consequently, such drawbacks lead to unsatisfied PDT effect.[17−21] Therefore, a new strategy is required to overcome these limitations of PDT.

Here, we fabricated PS-immobilized polyurethane (PU) polymer film to minimize side effects induced by injecting PS within the body. The PS-incorporated film was designed to induce generation of extracellular ROS under light irradiation. This platform that uses ROS-producing biomaterials enables localized delivery of ROS at the targeted site and timely production of ROS depending on irradiation. In addition, the amount of ROS generated is controlled by manipulating intensity and exposure time of light, and the amount of PS contained in the film.

In this study, we demonstrate the effect of extracellular ROS on vascular endothelial cell proliferation that can only be fulfilled by accurate control of optimum levels of ROS, and the merits of a new PDT system using PS-incorporated PU film to mediate local production of ROS.

2. EXPERIMENTAL SECTION

Preparation of Hp-Incorporated Polymer Film (Hp-PU Film). Hematoporphyrin (Hp), a harmless dye that has been widely used in PDT,[22,23] was purchased from Sigma-Aldrich (St. Louis, MO, USA). PU, a biocompatible polymer,[24] was selected because it is readily modified to suit a new PDT application to immobilize PS with a mixture of Hp, polymer, and solvent. Commercial medical-grade polyurethanes (Carbothane TPU PC3575A) were kindly supplied by Lubrizol (Wickliffe, OH, USA). The photofunctional PU film was manufactured using a solvent casting technique. The casting solution for the Hp-PU film was made by dissolving a fixed quantity of Hp with premixed 10% (w/v) PU in chloroform solvent (Sigma-Aldrich). The solvent was slowly evaporated at room temperature for 2 days in a fume hood. The dried film was punched into circular shapes, sterilized by soaking in 70% ethanol for 30 min. The specimens were then washed five times with distilled water and vacuum-dried for 48 h. All the samples were stored dry in a desiccator, wrapped in Al foils to prevent inadvertent photodegradation of film.

Photodynamic Treatment. A self-designed green light-emitting diode (LED) system was used as the light source to control PDT. The emission peak of the green LED light at 510 nm corresponds to the maximum absorption of Hp in the visible light region (Figure 1). This system was also designed with filters to cut off most ultraviolet radiation. The distance between the lamp and the sample is more than 5 cm. The power of irradiated light was measured with a power meter (S130C, Thorlab, Inc., USA) just before the experiment.

Characterization of the Hp-PU Film. Steady-state absorption and emission spectra were obtained using a UV−vis spectrophotometer (Hitachi, U-2900, Tokyo, Japan) and a spectrofluorimeter (Hitachi, F-4500, Tokyo, Japan), respectively. The distribution of Hp in the polymer matrix was observed by confocal microscopy (Carl Zeiss, LSM 700, NY, USA).

Detection of Singlet Oxygen and Total ROS Generated from the Hp-PU Film. Singlet oxygen generation was determined by measuring the phosphorescence signal from the de-excitation of singlet oxygen. The setup for the time and wavelength resolved singlet oxygen experiments was prepared as previously reported.[25−27] To prove total ROS generation, we measured degradation of 1,3-diphenyl-isobenzofuran (DPBF), a reactive oxygen quencher.[28] Briefly, 1 mL of ethanol solution containing the Hp-PU film and DPBF (1.85×10^{-5} M) was introduced into a 48-well plate in the dark. A green LED light source was used to irradiate the Hp-PU film and the

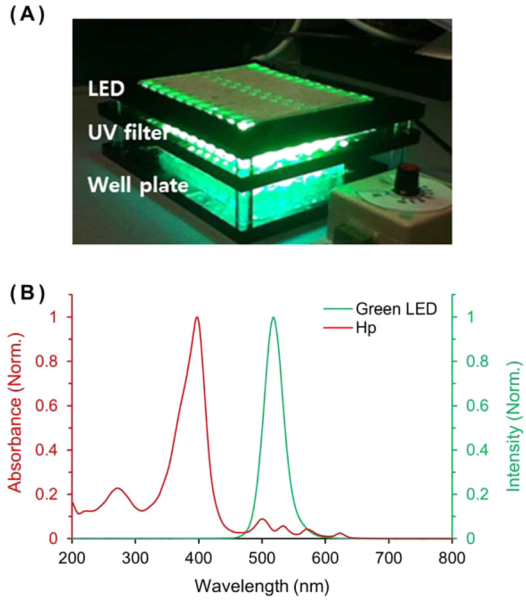

Figure 1. (A) Image of a self-designed green LED system. (B) Absorption spectra of Hp in ethanol (red line) and emission spectra of the green LED (green line).

LED power was 470 μW/cm^2. After every 10 min of irradiation, the O.D. of the DPBF absorption peak at 411 nm was monitored with a UV−vis spectrophotometer (Synergy H4, BioTek, VT, USA).

Measurement of Photodecomposition in the Hp-PU Film. First, absorbance of photosensitizer in the Hp-PU films, washed with 70% ethanol and distilled water, was obtained using a UV−vis spectrophotometer. Then, Hp-PU films were exposed with 470 μW/cm^2 for 45 min. After irradiation, absorbance of Hp in the film was remeasured. Photodecomposition of Hp is analyzed as the ratio between the O.D. values.

Cell Culture. Human umbilical vein endothelial cells (HUVECs) were purchased from Lonza (Basel, Switzerland) and maintained in endothelial basal medium-2 (EBM-2) with supplements (hEGF, FBS, VEGF, hFGF-B, hydrocortisone, GA-1000, R^3-IGF-1, heparin, and ascorbic acid; Lonza) at 37 °C in a 5% CO_2 incubator. HUVECs below passage 10 were used in this study.

Cell Proliferation Assay. HUVECs were seeded at a density of 2×10^4 cells per well onto the Hp-PU films. The cells were incubated for 24 h at 37 °C and then irradiated by green LED light. After irradiation, the cells were assayed for viability at different times (0, 1, and 3 days). Cells were incubated with 3-[4,5-dimethylthiazol-2-yl]-2,5-diphenyl tetrazolium bromide (MTT) solution (5 mg/mL) in EGM-2 (EBM-2 with supplements) for 4 h in the dark. Dimethyl sulfoxide was added to dissolve the formazan salts and the O.D. was measured at 570 nm.

Leaching Test. To check for efflux of Hp from the Hp-PU film, we placed the film in 500 μL of phosphate buffered saline (PBS) and media respectively for 72 h at 37 °C. Ethanol (1 mL) was added to the collected PBS. The O.D. of the ethanol was then measured by UV−vis spectrophotometer. Also, the collected media were treated in HUVECs cultured on 48-well plates. After 2 h, the media were discarded, replaced with 0.5 mL of fresh media and then irradiated by green LED light. Cell viability was measured by MTT at different times (0, 1, and 3 days).

Determination of Intracellular ROS Concentration. ROS concentrations in the cells were measured using an intracellular ROS assay kit (Cell Biolabs, Inc., San Diego, CA, USA). HUVECs were seeded at a density of 2×10^4 cells per well on the Hp-PU films and incubated for 24 h at 37 °C. Cells were preloaded with the 1 mM of the fluorescent dye 2,7-dichloro-dihydrofluorescein diacetate (DCFH-DA) for 1 h at 37 °C in the dark. The dye solution was removed and replaced with 0.5 mL of fresh media. Cells were exposed to light as

DOI: 10.1021/acsami.6b07628
ACS Appl. Mater. Interfaces 2016, 8, 28448−28457

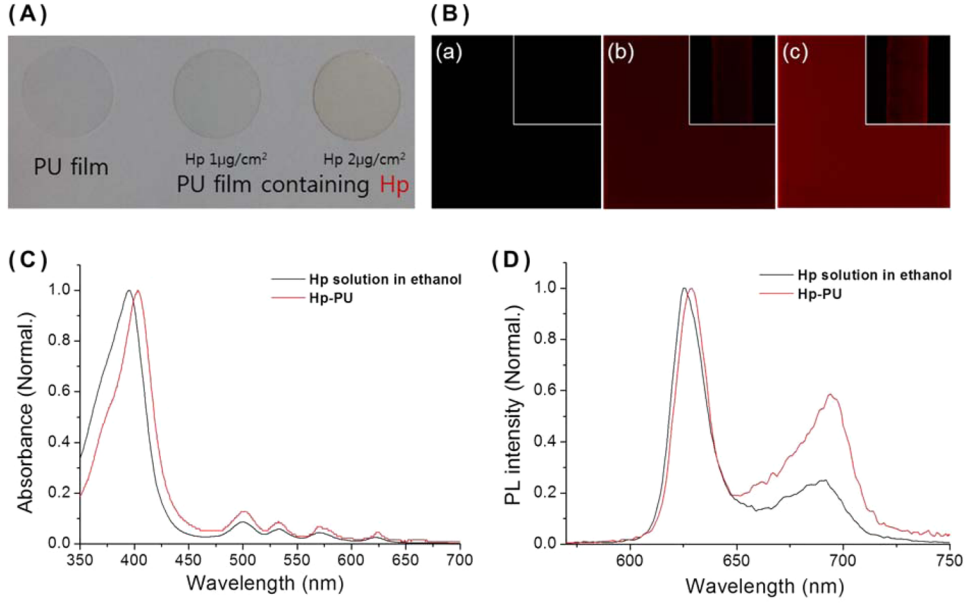

Figure 2. (A) 2D bare PU film and PU films containing Hp. (B) Fluorescence microscope image of (a) bare PU, (b) 1 μg/cm^2 Hp-PU film, and (c) 2 μg/cm^2 Hp-PU film (× 200, λ_{ex} = 405 nm, λ_{em} = 615 nm): the inset images show cross-sections of polymer films. (C) Steady-state absorption and (D) emission spectra of Hp in ethanol (black line) and of the Hp-PU (red line) are shown.

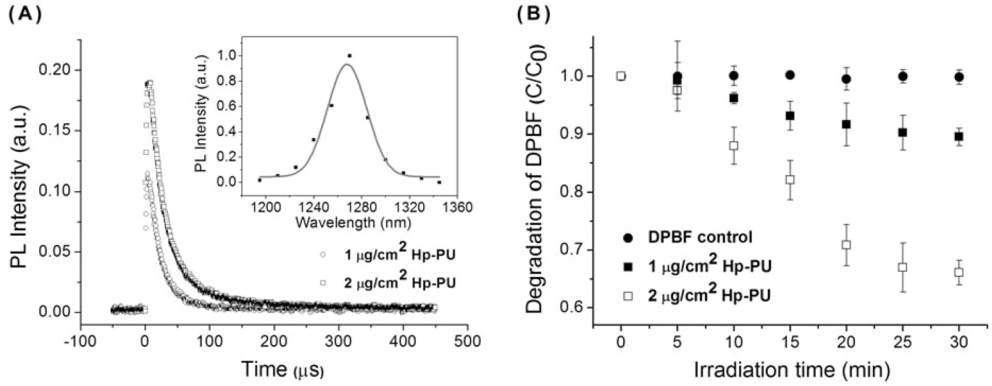

Figure 3. (A) Time-resolved singlet oxygen phosphorescence from the 1 μg/cm^2 Hp-PU film (black blank circle) and 2 μg/cm^2 Hp-PU film (black blank square) in PBS. The inset shows a Gaussian fitted singlet oxygen phosphorescence spectrum. (B) The ratio between the decomposition reaction O.D. (C) and the initial O.D. (C_0) of DPBF is shown as a function of irradiation time: DPBF only (black circle), DPBF with the 1 μg/cm^2 Hp-PU film (black square), and DPBF with the 2 μg/cm^2 Hp-PU film (blank square) under light exposure.

described above. After 24 h, the cells were washed three times with PBS and lysed by 0.1% triton X-100 in TE buffer (Tris-hydrochloride buffer, pH 8.0, containing 1.0 mM EDTA). The lysate was transferred to a 96-well black plate. Fluorescence was evaluated by UV−vis spectrophotometer by exciting the oxidized dichloro-fluorescein (DCF) product at 480 nm and measuring emission at 530 nm.

Suppression of Cell Proliferation with ROS Scavengers. To determine whether cell proliferation enhanced by PDT could be attributed to varying ROS concentrations within the cells, the cells were pretreated with either a free radical scavenger (5 mM N-acetyl cysteine, NAC)[29,30] or a singlet oxygen scavenger (10 μM sodium azide, NaN_3)[31,32] for 30 min at 37 °C. These agents were then replaced with fresh media and the cells were irradiated. Cell proliferation was assessed by MTT assay.

Cell Cycle Analysis. Cells were seeded at a density of 8 × 10^4 cells per well on the Hp-PU films in 12-well plates and incubated for 24 h at 37 °C. Light exposure was performed as described above. After incubation for 24 h, cells were treated with trypsin-EDTA and fixed in 70% ethanol for 1 h at −20 °C. The cells were washed with PBS and harvested by centrifugation. The resulting samples were incubated with RNase A (20 U/mL final concentration, Sigma) at 37 °C for 30 min. DNA was stained with 100 μg/mL propidium iodide (PI, Sigma) for 1 h in the dark. Cell cycle phase was determined in individual cells by fluorescence-activated cell sorting (BD FACS Verse) and subsequent analysis.

Western Blot Analysis. Proteins were separated by 12.5% SDS-polyacrylamide gel electrophoresis, and transferred to polyvinylidene difluoride (PVDF) membranes. Blots were incubated with a 1:1000 dilution of primary antibodies at 4 °C overnight, and then horseradish peroxidase (HRP)-linked anti-rabbit or anti-mouse IgG secondary antibodies (Cell signaling, MA, USA). The expressions of proteins were detected with the SinalFire ECL reagent (Cell signaling). The following primary antibodies were used: anti-Cyclin A2, anti-Cyclin E1, anti-CDK2 and anti-β-actin (Cell signaling).

BrdU-Immunochemistry. To estimate cells that enter S-phase, we performed BrdU-incorporation assay. HUVECs cultured on the PU films were irradiated by green LED light. Cells were incubated with a 5-bromo-2′-deoxyuridine (BrdU)-labeling solution for 2 h at 37 °C. Labeling medium was removed and the cells were then incubated with fixation solution for 30 min at room temperature. After fixation, anti-BrdU-POD working solution was added and immune complexes were detected by the substrate solution. The O.D. of the reaction product

DOI: 10.1021/acsami.6b07628
ACS Appl. Mater. Interfaces 2016, 8, 28448−28457

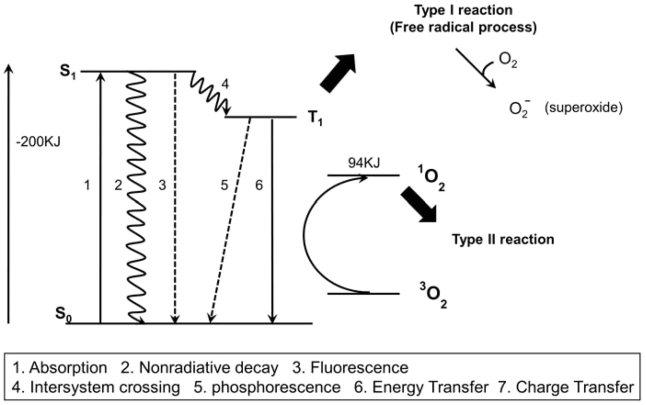

Figure 4. Schematic diagram of the photoinduced ROS generation mechanisms.

was measured at 370 nm with 492 nm reference wavelength using an automatic microplate reader (Spectra Max 340, Molecular Devices, Inc., Sunnyvale, CA, USA).

Nitrite Quantification. HUVECs were seeded at a density of 2×10^4 cells per well on the Hp-PU films, incubated for 24 h at 37 °C, and then irradiated. After additional incubation for 0, 1, and 3 days, accumulated nitrite in the culture medium was measured using a Griess reagent. Briefly, 50 μL of the supernatant was mixed with 100 μL of Griess reagent, 1% (w/v) sulfanilamide, and 0.1% (w/v) naphtylethylenediamine dihydrochloride in 5% (v/v) phosphoric acid. The mixture was incubated at room temperature for 10 min and the absorbance was measured by UV−vis spectrophotometer at 540 nm. Nitrite concentration was determined using a nitrite standard reference curve.

Statistical Analyses. All values are expressed as means ± the standard deviation of the mean. Differences between mean values of normally distributed data were assessed by Student's t tests. $P < 0.05$ was considered to be statistically significant.

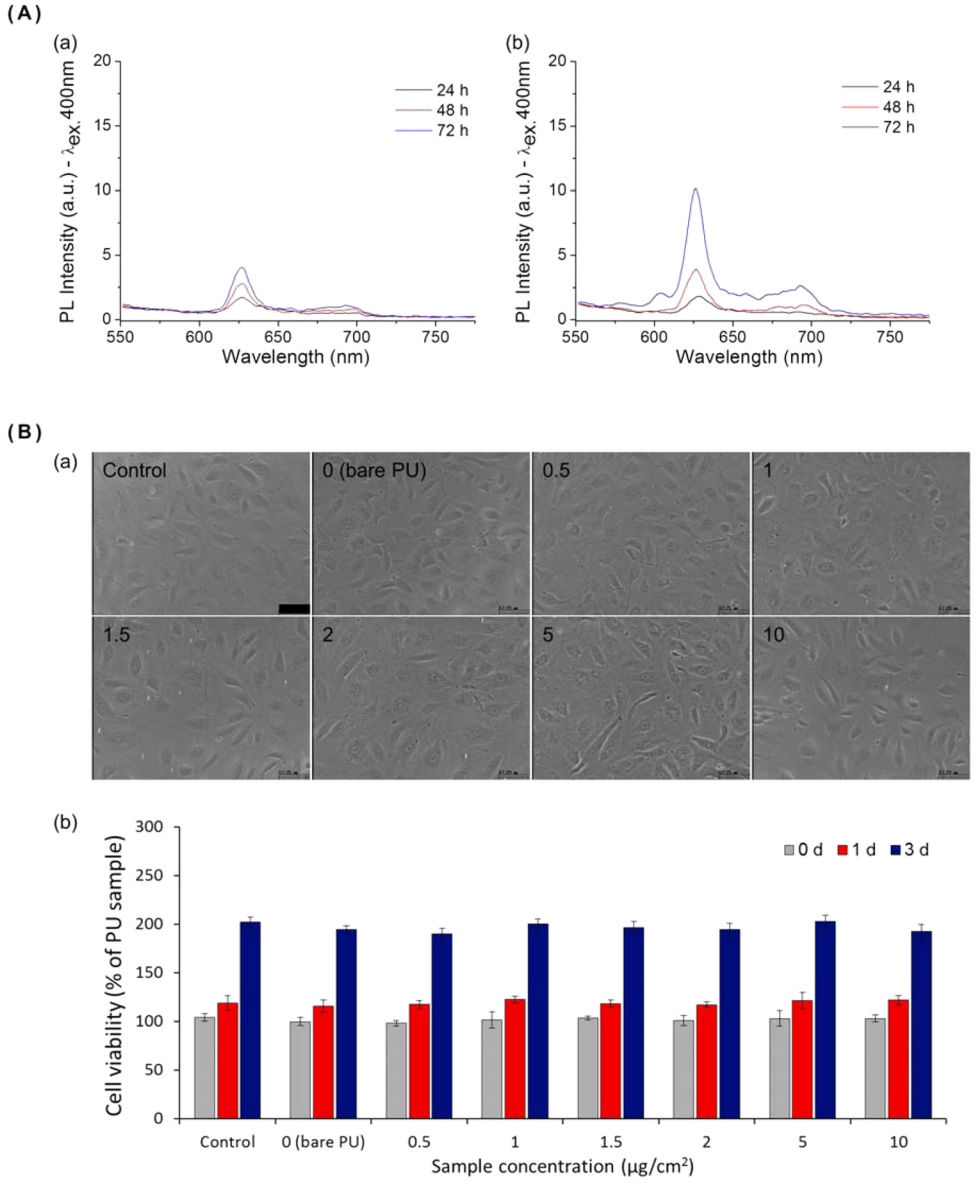

Figure 5. (A) Steady-state emission spectra of the leaching test solution, (a) 1 μg/cm^2 Hp-PU film and (b) 2 μg/cm^2 Hp-PU film for 72 h in PBS. (B) Cell viability with the leaching solution from bare, 0.5, 1, 1.5, 2, 5, and 10 μg/cm^2 Hp-PU films, (a) microscopic images of cell morphology (×200, scale bar: 67.25 μm) at 72 h after irradiation and (b) quantification of the number of viable cells by MTT assay for 72 h. Data are expressed as means ± SD, *$P < 0.05$ vs PU.

DOI: 10.1021/acsami.6b07628
ACS Appl. Mater. Interfaces 2016, 8, 28448−28457

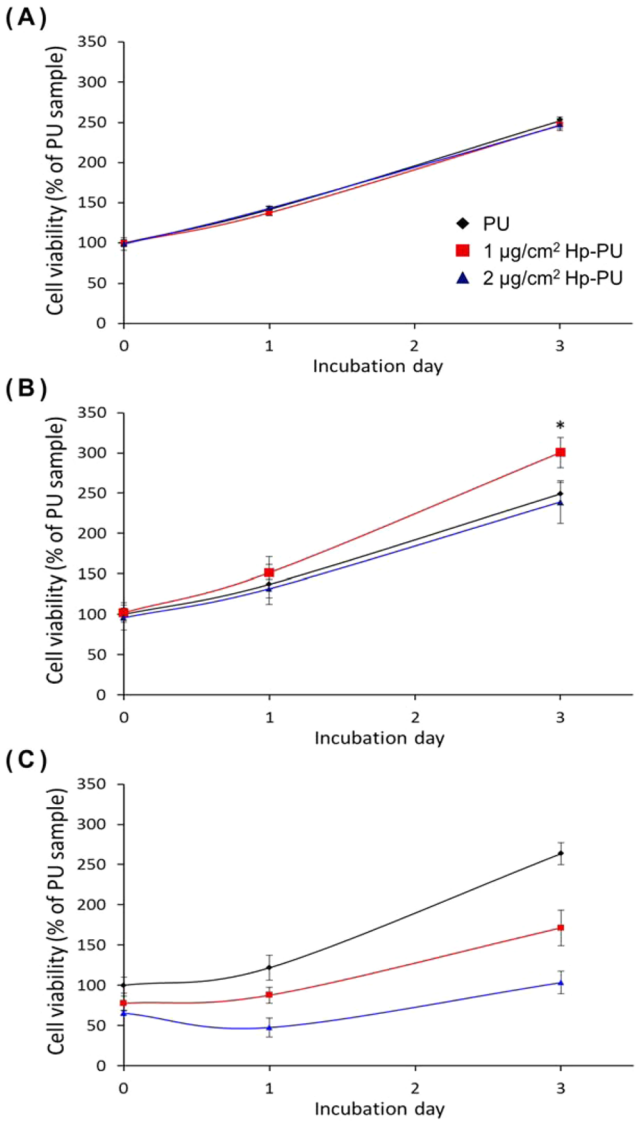

Figure 6. Effect of photodynamic treatment on cell proliferation measured by MTT. Cells were exposed with diverse light intensities for 30 min irradiation times, (A) 300 μW/cm^2, (B) 470 μW/cm^2, and (C) 3 mW/cm^2. Data are expressed as means ± SD, *P < 0.05 vs PU.

3. RESULTS AND DISCUSSION

Hp was incorporated into PU films at concentrations of 1 μg/cm^2 and 2 μg/cm^2 (Figure 2A). The thickness of Hp-PU films is 131.25 ± 6.41 μm. As shown in Figure 2Bb, c, the Hp was evenly embedded to the polymer matrix and the resulting fluorescence intensity depended on the concentration of embedded Hp. As shown in Figure. 2C, Hp in ethanol are two absorption regions of B band (395 nm) and Q bands (500, 533, 570, 622 nm). The absorption spectrum of Hp-PU film also contains the B and Q bands at similar wavelengths, but with slightly red-shifted peak positions. The difference in the peak position is possibly due to the vibrational energy state of Hp coupled with the polymer matrix and/or to self-coupling of Hp within the polymer matrix.[33,34] The steady-state fluorescence spectra (λ_{ex} = 405 nm) of Hp solution and Hp-PU film were normalized at their maximum peaks. The emission spectrum of Hp (λ_{ex} = 510 nm) solution in Figure 2D shows the two peaks at 625 and 690 nm, and the Hp-PU film presents the fluorescence spectrum with the small red shift and the change of the intensity ratio between the peaks as shown in the references.[33−36] The intensities of the absorption and emission spectra of the Hp-PU film depended on the concentration of Hp in the polymer matrix.

The most direct method of measuring singlet oxygen generation by Hp-PU film is to detect phosphorescence from the deactivation of singlet oxygen molecules induced by photoexcited Hp within the polymer matrix. The singlet oxygen phosphorescence signal from the Hp-PU film was measured in PBS at various detection wavelengths, between 1195 and 1345 nm (Figure 3A).[37] The phosphorescence decay signals were fitted to a single exponential function, resulting in 25 μs of decay time in the polymer matrix interfaced to PBS. Singlet oxygen was slow to decay due to the OH-free microenvironment.[38,39] However, decay of singlet oxygen generated by the Hp-PU film does not depend on the concentration of the photosensitizer, and intensity of the singlet oxygen phosphorescence depend on the concentration of the photosensitizer. Therefore, singlet oxygen generated by the Hp-PU film is proportionally increased along with the concentration of Hp (1 μg/cm^2: 2 μg/cm^2, 1:2.05). A decomposition study of DPBF was performed in Hp-PU films that generate total ROS upon green LED irradiation. DPBF is a ROS quencher and readily undergoes 1,4-cycloaddition reaction with singlet oxygen to form an endoperoxide that decomposes into an irreversible product (1,2-dibenzoylbenzene).[28] Reports suggest that DPBF is decomposed by a superoxide anion radical.[40,41] As shown in Figure 3B, the optical density (O.D.) of the DPBF absorption peak at 411 nm was not altered by irradiation with light (470 μW/cm^2 for 30 min), whereas the O.D. (C/C_0) of DPBF was reduced by the 1 μg/cm^2 and 2 μg/cm^2 Hp-PU film (10 ± 1.5% and 34 ± 3.1%, respectively) under irradiation. Thus, ROS generation by the Hp-PU film depends on the concentration of the Hp. These indicate that the interaction of light with Hp embedded PU film induces production of extracellular ROS, including both free radicals and singlet oxygen (nonradial ROS) through type I (charge transfer) and type II process (energy transfer), respectively, as shown in Figure 4.

To identify Hp-release profiles from Hp-PU film, the intrinsic fluorescence of Hp diffused into PBS (pH 7.4) was measured. The cumulative release at 72 h was 1.8 and 3.3% for the 1 and 2 μg/cm^2 Hp-PU films, respectively (Figure 5A). This experiment revealed that only small amounts of Hp were released into PBS due to our process immobilizing Hp on polymer film. Separately, to confirm effect of cell viability by cellular uptake of released Hp with light irradiation (5 mW/cm^2 for 30 min), the release of Hp was induced from the Hp-PU films of various concentrations into EGM-2 under the same conditions used in the previous experiment. Then, cells were treated with release media of Hp for 72 h. Although we used a high power density of light for the harsh environment, cell viability was not affected by interaction of released Hp with irradiation as compared with control (nontreatment) (Figure 5B). As mentioned above, classic PDT application injecting PS still has side effects which are mostly associated with low specificity of PS to targeting region. Therefore, these results suggest that a new PDT with Hp-immobilized PU films can minimize photosensitivity reaction caused by systemic administration of PS and increase the efficacy of localized treatment.

As mentioned above, it is known that a mild increase in the level of ROS play an important role in functioning as signaling molecules to enhance cellular growth.[2,8] The study was proceeded in vitro experiments to verify that the vascular endothelial cell proliferation was stimulated by precise modulation of

DOI: 10.1021/acsami.6b07628
ACS Appl. Mater. Interfaces 2016, 8, 28448−28457

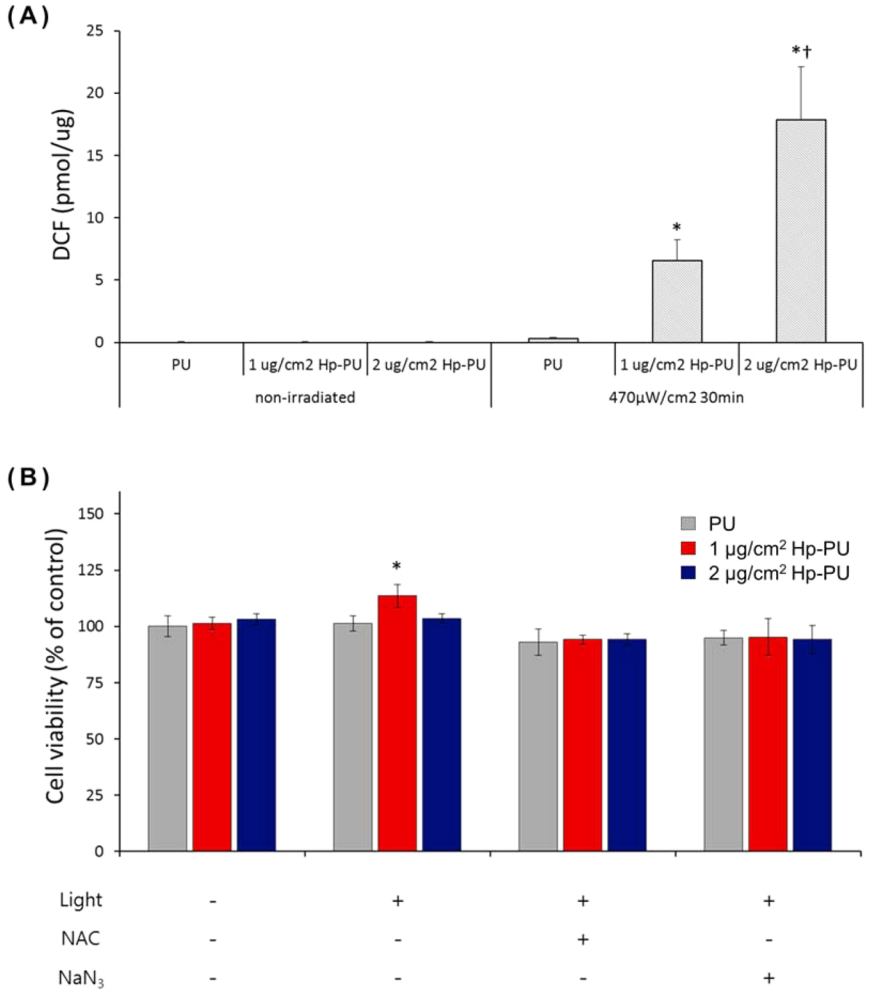

Figure 7. (A) Quantification of intracellular ROS accumulation with a DCFH-DA probe. (B) Antioxidant-mediated suppression of ROS generation and cell proliferation. Proliferation capacity in PDT-stimulated cells was determined with or without a preloading scavenger: 5 mM NAC or 10 μM NaN_3. Data are expressed as means ± SD, *P < 0.05 vs PU, †P < 0.05 vs 1 μg/cm^2 Hp-PU.

extracellular ROS based on Hp-PU film instead of endogenous ROS derived from cellular uptake of PS. PDT-induced cell proliferation was evaluated by MTT assay. HUVECs cultured on the Hp-PU film were exposed to a range of light intensities for 30 min. In accordance with previous reports that raising ROS levels above a critical threshold mediate cell damage,[9,42,43] these experiments showed that an increase in ROS resulted in significant cytotoxic effects to vascular endothelial cells. At intensities of 3 mW/cm^2 or greater, cell viability was reduced in an Hp-dose-dependent manner. However, cell proliferation is significantly enhanced by PDT-induced extracellular ROS from 1 μg/cm^2 Hp-PU films with 470 μW/cm^2 light intensity, compared to bare PU films. Exposure to light intensities of 300 μW/cm^2 or less caused no alteration to cell proliferation (Figure 6). This reveals that increased ROS within the extracellular environment affect cell growth. PDT used the Hp-PU film is a simple, but effective system that can modulate production rate of ROS by regulating the concentration of Hp and light irradiation condition. Besides, it should facilitate to control cellular behavior including cell proliferation or damage.

We hypothesized that increase of extracellular ROS might affect an environment in cells. First, to ascertain whether extracellular ROS induced a quantitative change in intracellular ROS, an oxidized DCF fluorescent probe was used to trace intracellular ROS production. At 24 h after 470 μW/cm^2 irradiation, PDT induced an Hp concentration-dependent increase in intracellular ROS accumulation (Figure 7A). As expected, extracellular ROS stimulated the formation of intracellular ROS. We also performed an experiment to verify whether a quantitative change in intracellular ROS is induced by cellular uptake of Hp released from the Hp-PU film under light irradiation. As a result, when cells were treated with Hp-contained media released for 72 h, intracellular ROS were not increased by uptake of Hp because only small amounts of Hp were released as already presented in Figure 5A (data not shown). Subsequently, to determine that ROS-stimulated cell proliferation is intracellular ROS-dependent, cell proliferation capacity was measured by MTT assay after preloading of intracellular ROS scavengers: NAC or NaN_3. The study was used two kinds of scavengers to investigate what specific types of ROS have positive effects on cell proliferation. When cells were exposed to 470 μW/cm^2 light intensity for 30 min, cell growth significantly increased on 1 μg/cm^2 Hp-PU films compared to the control. However, the observed proliferative effect was eliminated by treatment with scavengers (Figure 7B). These results indicate that extracellular ROS-induced cell proliferation correlates with a change in intracellular ROS accumulation. Also, we demonstrated that both singlet oxygen and free

DOI: 10.1021/acsami.6b07628
ACS Appl. Mater. Interfaces 2016, 8, 28448−28457

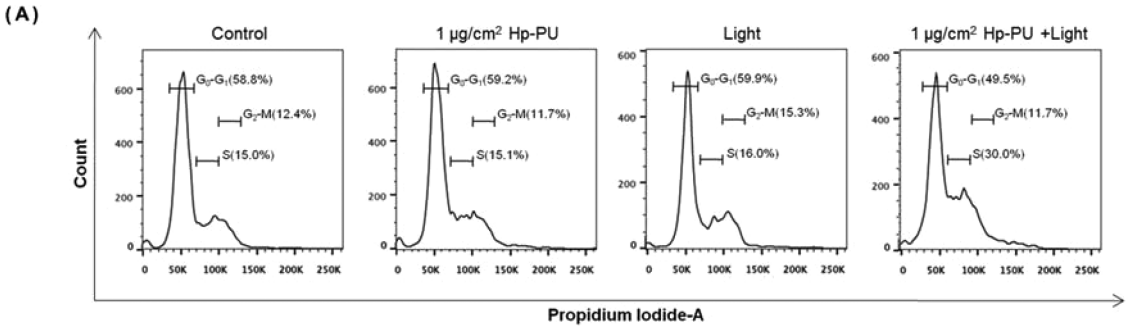

(B)

	Control	1 μg/cm² Hp-PU	Light	1 μg/cm² Hp-PU + Light
G0/G1 (%)	68.13±9.45	67.77±8.22	65.73±8.43	56.03±11.23
S (%)	**10.47±4.88**	**10.37±4.70**	**11.91±4.61**	**22.77±6.59**
G2/M (%)	12.13±1.72	12.53±2.65	13.97±1.74	12.56±4.08

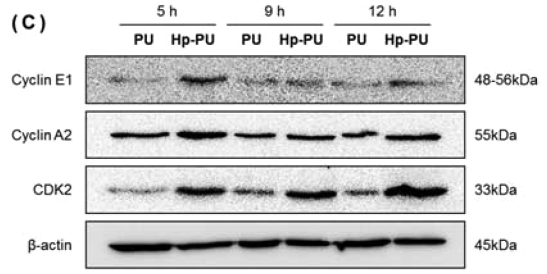

Figure 8. (A) Cell cycle analysis (24 h) was performed by flow cytometry. The groups were compared by cells grown on the control (PU film), the 1 μg/cm^2 Hp-PU film (nonirradiated), and those grown on the PU film + Light. (B) Table showing percentages of cells grown under the specified conditions at a specific phase in the cell cycle. Data are expressed as means ± SD from three experiments performed in triplicate. (C) Expression of cell cycle regulatory proteins in lysate (40 μg/lane) was analyzed by Western blot at different time points (5, 9, 12 h after irradiation). β-actin was used as a loading control. Hp-PU: 1 μg/cm^2 Hp-PU film.

radical affect the growth of endothelial cells by PDT with Hp-incorporated PU film. ROS vary in their inherent reactivities, stability, and diffusibility.[44] It is known that Hydrogen peroxide (H_2O_2) can diffuse through specific aquaporins (AQP) in the plasma membrane, superoxide anion ($O2^-$) also can initiate intracellular signaling by permeation across the cell membrane through anion channels (Cl^- channel-3).[45−47] However, it is still unclear whether PDT-induced extracellular ROS diffuse in the plasma membrane or trigger receptor-mediated or mitochondria-mediated pathways by oxidative stress in endothelial cell. Previous studies have reported that low extracellular ROS dose can increase production of growth factors such as vascular endothelial growth factor (VEGF) and fibroblast growth factor-2 (FGF-2),[3,48,49] as well as insulin-like growth factor-1 (IGF-1).[50] Specially, it has been known that epidermal growth factor (EGF) and other growth factors bind to its specific receptor and can induce release of intracellular ROS, and the released ROS may contribute to cell proliferation through activation of Akt and mitogen-activated protein kinases (MAPKs) signaling pathway.[4,51,52] Therefore, we supposed that extracellular ROS are the essential mediator for intracellular ROS-induced cell proliferation through growth factor-related mechanisms.

As mentioned above, ROS mediate a variety of cellular signaling pathways and exogenous ROS are known to directly initiate signaling responses. Previous studies have reported that exogenous ROS induce the activation of extracellular signal regulated kinase (ERK), c-Jun N-terminal kinases (JNK), p38 MAPKs, and Akt.[53,54] The classical ERK family (p42/44 MAPK) and JNK are known for an intracellular checkpoint for cellular mitogenesis and the ERK cascade plays a key role in the control of cell cycle progression.[55] Cells are duplicated by a process known as the cell cycle.[56] At the stages of the cell cycle, replication of DNA occurs during a specific part of the interphase called S phase.[57] The transition from G1 to S phase of the cell cycle is critical for controlling cell proliferation.[58]

We thus speculated that cell proliferation promoted by PDT is associated with acceleration of the G1/S phase transition. Indeed, after light irradiation, the S phase cell population was remarkably increased in the cell-proliferative condition (1 μg/cm^2 Hp-PU film + light) compared to the control (Figure 8A and B). Without irradiation, cells grown on the Hp-PU film did not produce a significant change in the cell cycle population. The Cyclin family of cell cycle regulator proteins is important for the redox-dependent regulation of cell cycle progression.[9] Cyclins and their partners the cyclin dependent kinases (CDK) act at a different step of the cell cycle; CDK4-Cyclin D complexes lead to entering into G1 phase.[57,59−61] In particular, cell proliferation is controlled by CDK2 which in association with Cyclin E and Cyclin A regulates G1/S transition and S phase progression, respectively.[55,62] On the basis of the above results using FACS, we hypothesized that the stimulation of cell proliferation and the increase in the mitotic index after PDT was closely linked to an accompanying expression of cell cycle regulatory proteins. To confirm this assumption we conducted a time course analysis of CDK and Cyclin protein expression with Western blot after irradiation. This data shown a transient up-regulation of Cyclin E1 protein levels expressed during the G1/S transition at 5 h in the cell-proliferative condition. Also, the expression of Cyclin A2 and CDK2 appearing in S phase were significantly increased by enhancing ROS between 5 and 12 h (Figure 8C). As a result, our studies indicate that the stimulation of cell proliferation by ROS is associated with an increased expression of cell cycle regulatory proteins related S phase, and extracellular ROS could trigger the molecular mechanism that control cell cycle regulation, leading to cell proliferation.

In addition, we also evaluated that the mitogenic effect of PDT with Hp-PU films through a two-step irradiation. Before and after light irradiation, the difference of absorbance of intrinsic Hp at 500 nm was within measurement error of absorption

DOI: 10.1021/acsami.6b07628
ACS Appl. Mater. Interfaces 2016, 8, 28448−28457

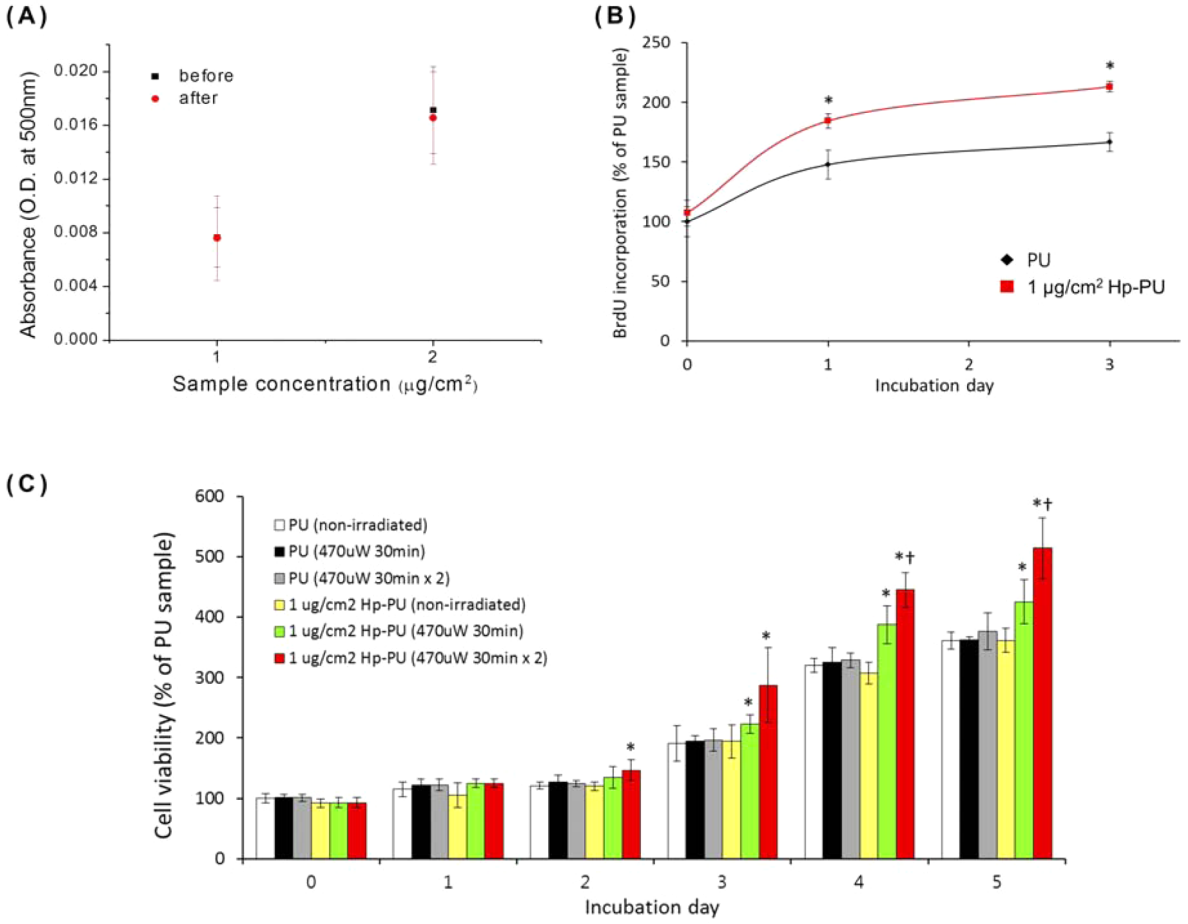

Figure 9. (A) Photostability of a photosensitizer in the Hp-PU film with a single irradiation. (B) Mitogenic effect of PDT (470 μW/cm^2 for 30 min) quantified by BrdU immunochemistry. (C) Stimulation of cell proliferation by additional irradiation at 48 h after the first treatment. Data are expressed as means ± SD, *P < 0.05 vs PU, †P < 0.05 vs a single irradiation.

spectrophotometer (photometric accuracy: ± 0.002Abs, 0 to 0.5 Abs) (Figure 9A). Thus, continuous PDT was designed because Hp-PU film was not photodecomposed by a single irradiation. Although the number of BrdU-immunoreactive cells was increased by about 22% between 1 μg/cm^2 Hp-PU films and bare PU films with 470 μW/cm^2, the ratio of increased mitotic precursors was decreased after 24 h of light exposure (Figure 9B). Our result showed that cell growth was steadily increased through a second irradiation at 48 h in the same conditions, enhanced cell proliferation and mitotic ratio, as compared to a single irradiation (Figure 9C). As a whole, these results demonstrate that Hp-PU films should facilitate a two-step PDT, resulting in an additional increase of endothelial cell proliferation.

A primary function of vascular endothelial cells is to secrete products that prevent clotting and inhibit vascular smooth muscle cell (VSMC) proliferation. Nitric oxide (NO) is a predominant antithrombogenic and antiproliferative agent in VSMCs.[63,64] The NO secretion rate of HUVECs grown on Hp-PU film did not change compared to that of cells grown on bare PU films after irradiation (Figure 10). Consequently, low levels of ROS generated by PDT did not negatively affect the function of proliferated cells.

In this study, we have demonstrated that the PDT platform using the photofunctional materials, an Hp-incorporated PU film, can be an effective strategy to enhance cell proliferation by optimizing the generation of extracellular ROS without cellular uptake of photosensitizer. Specially, in vascular endothelial cells, the stimulation of ROS-induced cell growth may also be used a therapeutic method to overcome synthetic vascular graft failures caused mainly by thrombosis and intimal hyperplasia, which is prevented by the rapid re-endothelialization in graft.

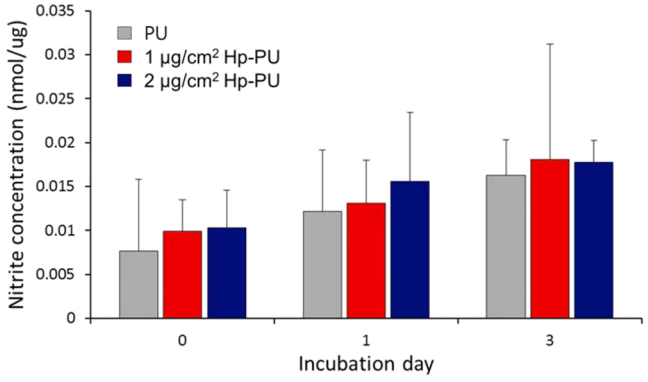

Figure 10. Confirmation of NO secretory ability in proliferated cells by PDT. Nitrite that accumulated in the culture medium was measured with a Griess reaction after 470 μW/cm^2 for 30 min.

4. CONCLUSION

We have designed hematoporphyrin-incorporated polymer films which produce extracellular ROS under light irradiation

DOI: 10.1021/acsami.6b07628
ACS Appl. Mater. Interfaces 2016, 8, 28448−28457

to avert cellular uptake of ROS-inducing agents. This platform was used to control the generation of ROS and to facilitate localized delivery of ROS to specific lesions via regulating parameters such as the intensity and exposure time of light, and the amount of PS contained in the film. In vascular endothelial cells, a modified PDT based on 1 $\mu g/cm^2$ Hp-PU films is effectively enhanced cell growth with irradiation of 470 $\mu W/cm^2$ 30 min. We also found that extracellular ROS mediate the formation of intracellular ROS, and a moderate increase in intracellular ROS contributes considerably to endothelial cell proliferation, followed by a concomitant expression of cell cycle regulatory proteins which associate with G1/S transition and S phase progression. We believe that new PDT system, established by incorporating PS into PU polymer film, can improve the therapeutic efficacy by localized delivery of extracellular ROS while reducing undesired side effects caused by systemic administration of PS. Furthermore, this approach that controls endothelial cell growth is expected to be a potential strategy for the design of next generation PDT.

AUTHOR INFORMATION

Corresponding Authors

*E-mail: yrkim@yonsei.ac.kr. Tel: 82-2-2123-2646. Fax: 82-2-364-7050.

*E-mail: parkjc@yuhs.ac. Tel: 82-2-2228-1917. Fax: 82-2-363-9923.

Author Contributions

[‖]M.-A.K. and B.-J.K. contributed equally. The manuscript was written through contributions of all authors. All authors have given approval to the final version of the manuscript.

Notes

The authors declare no competing financial interest.

ACKNOWLEDGMENTS

This research was supported by the National Research Foundation of Korea (NRF) funded by the Ministry of Science, ICT & Future Planning(Grant 2012-049729).

REFERENCES

(1) Circu, M. L.; Aw, T. Y. Reactive Oxygen Species, Cellular Redox Systems, and Apoptosis. *Free Radical Biol. Med.* **2010**, *48*, 749−762.

(2) Trachootham, D.; Alexandre, J.; Huang, P. Targeting Cancer Cells by ROS-Mediated Mechanisms: A Radical Therapeutic Approach? *Nat. Rev. Drug Discovery* **2009**, *8*, 579−591.

(3) Arjunan, K. P.; Friedman, G.; Fridman, A.; Clyne, A. M. Non-Thermal Dielectric Barrier Discharge Plasma Induces Angiogenesis through Reactive Oxygen Species. *J. R. Soc., Interface* **2012**, *9*, 147−157.

(4) Huo, Y.; Qiu, W. Y.; Pan, Q.; Yao, Y. F.; Xing, K.; Lou, M. F. Reactive Oxygen Species (ROS) Are Essential Mediators in Epidermal Growth Factor (EGF)-Stimulated Corneal Epithelial Cell Proliferation, Adhesion, Migration, and Wound Healing. *Exp. Eye Res.* **2009**, *89*, 876−886.

(5) Panieri, E.; Gogvadze, V.; Norberg, E.; Venkatesh, R.; Orrenius, S.; Zhivotovsky, B. Reactive Oxygen Species Generated in Different Compartments Induce Cell Death, Survival, or Senescence. *Free Radical Biol. Med.* **2013**, *57*, 176−187.

(6) Schafer, F. Q.; Buettner, G. R. Redox Environment of the Cell as Viewed through the Redox State of the Glutathione Disulfide/Glutathione Couple. *Free Radical Biol. Med.* **2001**, *30*, 1191−1212.

(7) Han, Y.; Huang, C.; Sun, X.; Xiang, B.; Wang, M.; Yeh, E. T.; Chen, Y.; Li, H.; Shi, G.; Cang, H.; Sun, Y.; Wang, J.; Wang, W.; Gao, F.; Yi, J. SENP3-Mediated De-Conjugation of SUMO2/3 from Promyelocytic Leukemia Is Correlated with Accelerated Cell Proliferation under Mild Oxidative Stress. *J. Biol. Chem.* **2010**, *285*, 12906−12915.

(8) Dandapat, A.; Hu, C.; Sun, L.; Mehta, J. L. Small Concentrations of OxLDL Induce Capillary Tube Formation from Endothelial Cells Via LOX-1-Dependent Redox-Sensitive Pathway. *Arterioscler., Thromb., Vasc. Biol.* **2007**, *27*, 2435−2442.

(9) Blazquez-Castro, A.; Carrasco, E.; Calvo, M. I.; Jaen, P.; Stockert, J. C.; Juarranz, A.; Sanz-Rodriguez, F.; Espada, J. Protoporphyrin IX-Dependent Photodynamic Production of Endogenous ROS Stimulates Cell Proliferation. *Eur. J. Cell Biol.* **2012**, *91*, 216−223.

(10) Huang, P.; Lin, J.; Wang, X.; Wang, Z.; Zhang, C.; He, M.; Wang, K.; Chen, F.; Li, Z.; Shen, G.; Cui, D.; Chen, X. Light-Triggered Theranostics Based on Photosensitizer-Conjugated Carbon Dots for Simultaneous Enhanced-Fluorescence Imaging and Photodynamic Therapy. *Adv. Mater.* **2012**, *24*, 5104−5110.

(11) Robertson, C. A.; Evans, D. H.; Abrahamse, H. Photodynamic Therapy (PDT): A Short Review on Cellular Mechanisms and Cancer Research Applications for PDT. *J. Photochem. Photobiol., B* **2009**, *96*, 1−8.

(12) Zhang, D.; Wu, M.; Zeng, Y.; Wu, L.; Wang, Q.; Han, X.; Liu, X.; Liu, J. Chlorin E6 Conjugated Poly(Dopamine) Nanospheres as Pdt/Ptt Dual-Modal Therapeutic Agents for Enhanced Cancer Therapy. *ACS Appl. Mater. Interfaces* **2015**, *7*, 8176−8187.

(13) Aluigi, A.; Sotgiu, G.; Torreggiani, A.; Guerrini, A.; Orlandi, V. T.; Corticelli, F.; Varchi, G. Methylene Blue Doped Films of Wool Keratin with Antimicrobial Photodynamic Activity. *ACS Appl. Mater. Interfaces* **2015**, *7*, 17416−17424.

(14) Dolmans, D. E. J. G. J.; Fukumura, D.; Jain, R. K. Photodynamic Therapy for Cancer. *Nat. Rev. Cancer* **2003**, *3*, 380−387.

(15) Moor, A. C. E. Signaling Pathways in Cell Death and Survival after Photodynamic Therapy. *J. Photochem. Photobiol., B* **2000**, *57*, 1−13.

(16) Huang, L.; Xuan, Y.; Koide, Y.; Zhiyentayev, T.; Tanaka, M.; Hamblin, M. R. Type I and Type II Mechanisms of Antimicrobial Photodynamic Therapy: An in Vitro Study on Gram-Negative and Gram-Positive Bacteria. *Lasers Surg. Med.* **2012**, *44*, 490−499.

(17) Liang, R.; Tian, R.; Ma, L.; Zhang, L.; Hu, Y.; Wang, J.; Wei, M.; Yan, D.; Evans, D. G.; Duan, X. A Supermolecular Photosensitizer with Excellent Anticancer Performance in Photodynamic Therapy. *Adv. Funct. Mater.* **2014**, *24*, 3144−3151.

(18) Nishiyama, N.; Morimoto, Y.; Jang, W.-D.; Kataoka, K. Design and Development of Dendrimer Photosensitizer-Incorporated Polymeric Micelles for Enhanced Photodynamic Therapy. *Adv. Drug Delivery Rev.* **2009**, *61*, 327−338.

(19) Wang, S.; Huang, P.; Nie, L.; Xing, R.; Liu, D.; Wang, Z.; Lin, J.; Chen, S.; Niu, G.; Lu, G.; Chen, X. Single Continuous Wave Laser Induced Photodynamic/Plasmonic Photothermal Therapy Using Photosensitizer-Functionalized Gold Nanostars. *Adv. Mater.* **2013**, *25*, 3055−3061.

(20) Chen, Z.; Li, Z.; Wang, J.; Ju, E.; Zhou, L.; Ren, J.; Qu, X. A Multi-Synergistic Platform for Sequential Irradiation-Activated High-Performance Apoptotic Cancer Therapy. *Adv. Funct. Mater.* **2014**, *24*, 522−529.

(21) Gong, H.; Cheng, L.; Xiang, J.; Xu, H.; Feng, L.; Shi, X.; Liu, Z. Near-Infrared Absorbing Polymeric Nanoparticles as a Versatile Drug Carrier for Cancer Combination Therapy. *Adv. Funct. Mater.* **2013**, *23*, 6059−6067.

(22) Tang, W.; Liu, Q.; Wang, X.; Wang, P.; Zhang, J.; Cao, B. Potential Mechanism in Sonodynamic Therapy and Focused Ultrasound Induced Apoptosis in Sarcoma 180 Cells in Vitro. *Ultrasonics* **2009**, *49*, 786−793.

(23) Ren, Y.; Wang, R.; Liu, Y.; Guo, H.; Zhou, X.; Yuan, X.; Liu, C.; Tian, J.; Yin, H.; Wang, Y.; Zhang, N. A Hematoporphyrin-Based Delivery System for Drug Resistance Reversal and Tumor Ablation. *Biomaterials* **2014**, *35*, 2462−2470.

(24) Guelcher, S. A. Biodegradable Polyurethanes: Synthesis and Applications in Regenerative Medicine. *Tissue Eng., Part B* **2008**, *14*, 3−17.

DOI: 10.1021/acsami.6b07628
ACS Appl. Mater. Interfaces 2016, 8, 28448−28457

(25) Wang, K.-K.; Jung, M.-S.; Choi, K.-H.; Shin, H.-W.; Oh, S.-I.; Im, J.-E.; Kim, D.-H.; Kim, Y.-R. Fabrication and Photophysical Properties of Singlet Oxygen Generating Nanoporous Membrane. *Surf. Coat. Technol.* **2011**, *205*, 3905−3908.
(26) Wang, K.-K.; Kim, B.-J.; Lee, M. H.; Kwon, B.-J.; Choi, D. H.; Park, J.-C.; Kim, Y.-R. Photofunctional Co-Cr Alloy Generating Reactive Oxygen Species for Photodynamic Applications. *Int. J. Photoenergy* **2013**, *2013*, 1−8.
(27) Wang, K.-K.; Jung, S.-J.; Hwang, J.-W.; Kim, B.-J.; Kim, D.-H.; Bae, I.-K.; Jeong, S. H.; Kim, Y.-R. Bactericidal Effect through Non-Uptake Pathway with Photofunctional Silicon Polymer That Generates Reactive Oxygen Species. *J. Photochem. Photobiol., A* **2016**, *315*, 52−58.
(28) Zhang, X.-F.; Li, X. The Photostability and Fluorescence Properties of Diphenylisobenzofuran. *J. Lumin.* **2011**, *131*, 2263−2266.
(29) Zhou, H.; Randers-Pehrson, G.; Waldren, C. A.; Hei, T. K. Radiation-Induced Bystander Effect and Adaptive Response in Mammalian Cells. *Adv. Space Res.* **2004**, *34*, 1368−1372.
(30) Shen, W. L.; Gao, P. J.; Che, Z. Q.; Ji, K. D.; Yin, M.; Yan, C.; Berk, B. C.; Zhu, D. L. NAD(P)H Oxidase-Derived Reactive Oxygen Species Regulate Angiotensin-II Induced Adventitial Fibroblast Phenotypic Differentiation. *Biochem. Biophys. Res. Commun.* **2006**, *339*, 337−343.
(31) Kishimoto, S.; Bernardo, M.; Saito, K.; Koyasu, S.; Mitchell, J. B.; Choyke, P. L.; Krishna, M. C. Evaluation of Oxygen Dependence on in Vitro and in Vivo Cytotoxicity of Photoimmunotherapy Using IR-700-Antibody Conjugates. *Free Radical Biol. Med.* **2015**, *85*, 24−32.
(32) Kusano, S.; Haruyama, T.; Ishiyama, S.; Hagihara, S.; Nagatsugi, F. Development of the Crosslinking Reactions to RNA Triggered by Oxidation. *Chem. Commun. (Cambridge, U. K.)* **2014**, *50*, 3951−3954.
(33) Holland, B. T.; Walkup, C.; Stein, A. Encapsulation, Stabilization, and Catalytic Properties of Flexible Metal Porphyrin Complexes in MCM-41 with Minimal Electronic Perturbation by the Environment. *J. Phys. Chem. B* **1998**, *102*, 4301−4309.
(34) Subbiah, S.; Mokaya, R. Synthesis of Transparent and Ordered Mesoporous Silica Monolithic Films Embedded with Monomeric Zinc Phthalocyanine Dye. *Chem. Commun. (Cambridge, U. K.)* **2003**, 860−861.
(35) Yamazaki, T.; Yamazaki, I.; Osuko, A. Photoinduced Electron Transfer and Molecular Orientation of Zinc Porphyrin-Imide Dyads in Langmuir-Blodgett Monolayer Films. *J. Phys. Chem. B* **1998**, *102*, 7858−7865.
(36) Wu, C.; McNeill, J. Swelling-Controlled Polymer Phase and Fluorescence Properties of Polyfluorene Nanoparticles. *Langmuir* **2008**, *24*, 5855−5861.
(37) Choi, K. H.; Lee, H. J.; Park, B. J.; Wang, K. K.; Shin, E. P.; Park, J. C.; Kim, Y. K.; Oh, M. K.; Kim, Y. R. Photosensitizer and Vancomycin-Conjugated Novel Multifunctional Magnetic Particles as Photoinactivation Agents for Selective Killing of Pathogenic Bacteria. *Chem. Commun. (Cambridge, U. K.)* **2012**, *48*, 4591−4593.
(38) Manjon, F.; Santana-Magana, M.; Garcia-Fresnadillo, D.; Orellana, G. Singlet Oxygen Sensitizing Materials Based on Porous Silicone: Photochemical Characterization, Effect of Dye Reloading and Application to Water Disinfection with Solar Reactors. *Photochem. Photobiol. Sci.* **2010**, *9*, 838−845.
(39) Manjón, F.; Villén, L.; García-Fresnadillo, D.; Orellana, G. On the Factors Influencing the Performance of Solar Reactors for Water Disinfection with Photosensitized Singlet Oxygen. *Environ. Sci. Technol.* **2008**, *42*, 301−307.
(40) Ohyashiki, T.; Nunomura, M.; Katoh, T. Detection of Superoxide Anion Radical in Phospholipid Liposomal Membrane by Fluorescence Quenching Method Using 1,3-Diphenylisobenzofuran. *Biochim. Biophys. Acta, Biomembr.* **1999**, *1421*, 131−139.
(41) Gomes, A.; Fernandes, E.; Lima, J. L. Fluorescence Probes Used for Detection of Reactive Oxygen Species. *J. Biochem. Biophys. Methods* **2005**, *65*, 45−80.
(42) Buytaert, E.; Dewaele, M.; Agostinis, P. Molecular Effectors of Multiple Cell Death Pathways Initiated by Photodynamic Therapy. *Biochim. Biophys. Acta, Rev. Cancer* **2007**, *1776*, 86−107.
(43) Oleinick, N. L.; Morris, R. L.; Belichenko, I. The Role of Apoptosis in Response to Photodynamic Therapy: What, Where, Why, and How. *Photochem. Photobiol. Sci.* **2002**, *1*, 1−21.
(44) Waghray, M.; Cui, Z.; Horowitz, J. C.; Subramanian, I. M.; Martinez, F. J.; Toews, G. B.; Thannickal, V. J. Hydrogen Peroxide Is a Diffusible Paracrine Signal for the Induction of Epithelial Cell Death by Activated Myofibroblasts. *FASEB J.* **2005**, *19*, 854−856.
(45) Fisher, A. B. Redox Signaling across Cell Membranes. *Antioxid. Redox Signaling* **2009**, *11*, 1349−1356.
(46) Dickinson, B. C.; Chang, C. J. Chemistry and Biology of Reactive Oxygen Species in Signaling or Stress Responses. *Nat. Chem. Biol.* **2011**, *7*, 504−511.
(47) Sies, H. Role of Metabolic H_2O_2 Generation: Redox Signaling and Oxidative Stress. *J. Biol. Chem.* **2014**, *289*, 8735−8741.
(48) Sen, C. K.; Khanna, S.; Babior, B. M.; Hunt, T. K.; Ellison, E. C.; Roy, S. Oxidant-Induced Vascular Endothelial Growth Factor Expression in Human Keratinocytes and Cutaneous Wound Healing. *J. Biol. Chem.* **2002**, *277*, 33284−33290.
(49) Black, S. M.; DeVol, J. M.; Wedgwood, S. Regulation of Fibroblast Growth Factor-2 Expression in Pulmonary Arterial Smooth Muscle Cells Involves Increased Reactive Oxygen Species Generation. *Am. J. Physiol. Cell Physiol.* **2008**, *294*, C345−354.
(50) Delafontaine, P.; Ku, L. Reactive Oxygen Species Stimulate Insulin-Like Growth Factor I Synthesis in Vascular Smooth Muscle Cells. *Cardiovasc. Res.* **1997**, *33*, 216−222.
(51) Bae, Y. S.; Kang, S. W.; Seo, M. S.; Baines, I. C.; Tekle, E.; Chock, P. B.; Rhee, S. G. Epidermal Growth Factor (EGF)-Induced Generation of Hydrogen Peroxide. Role in EGF Receptor-Mediated Tyrosine Phosphorylation. *J. Biol. Chem.* **1997**, *272*, 217−221.
(52) Lo, Y. Y. C.; Cruz, T. F. Involvement of Reactive Oxygen Species in Cytokine and Growth Factor Induction of c-Fos Expression in Chondrocytes. *J. Biol. Chem.* **1995**, *270*, 11727−11730.
(53) Chen, K.; Kirber, M. T.; Xiao, H.; Yang, Y.; Keaney, J. F., Jr. Regulation of ROS Signal Transduction by NADPH Oxidase 4 Localization. *J. Cell Biol.* **2008**, *181*, 1129−1139.
(54) Thomas, S. R.; Chen, K.; Keaney, J. F., Jr. Hydrogen Peroxide Activates Endothelial Nitric-Oxide Synthase through Coordinated Phosphorylation and Dephosphorylation Via a Phosphoinositide 3-Kinase-Dependent Signaling Pathway. *J. Biol. Chem.* **2002**, *277*, 6017−6024.
(55) Zhang, W.; Liu, H. T. MAPK Signal Pathways in the Regulation of Cell Proliferation in Mammalian Cells. *Cell Res.* **2002**, *12*, 9−18.
(56) Boonstra, J.; Post, J. A. Molecular Events Associated with Reactive Oxygen Species and Cell Cycle Progression in Mammalian Cells. *Gene* **2004**, *337*, 1−13.
(57) Vermeulen, K.; Van Bockstaele, D. R.; Berneman, Z. N. The Cell Cycle: A Review of Regulation, Deregulation and Therapeutic Targets in Cancer. *Cell Proliferation* **2003**, *36*, 131−149.
(58) Bertoli, C.; Skotheim, J. M.; de Bruin, R. A. Control of Cell Cycle Transcription During G1 and S Phases. *Nat. Rev. Mol. Cell Biol.* **2013**, *14*, 518−528.
(59) Ledda-Columbano, G. M.; Pibiri, M.; Loi, R.; Perra, A.; Shinozuka, H.; Columbano, A. Early Increase in Cyclin-D1 Expression and Accelerated Entry of Mouse Hepatocytes into S Phase after Administration of the Mitogen 1,4-Bis[2-(3,5-Dichloropyridyloxy)] Benzene. *Am. J. Pathol.* **2000**, *156*, 91−97.
(60) Pines, J. Cyclins and Cyclin-Dependent Kinases: A Biochemical View. *Biochem. J.* **1995**, *308* (Pt3), 697−711.
(61) Sherr, C. J. Cancer Cell Cycles. *Science* **1996**, *274*, 1672−1677.
(62) Alisi, A.; Spagnuolo, S.; Leoni, S. Treatment with EGF Increases the Length of S-Phase after Partial Hepatectomy in Rat, Changing the Activities of Cdks. *Cell. Physiol. Biochem.* **2003**, *13*, 239−248.
(63) Rzucidlo, E. M.; Martin, K. A.; Powell, R. J. Regulation of Vascular Smooth Muscle Cell Differentiation. *J. Vasc. Surg.* **2007**, *45*, A25−A32.
(64) McCormick, C.; Wadsworth, R. M.; Jones, R. L.; Kennedy, S. Prostacyclin Analogues: The Next Drug-Eluting Stent? *Biochem. Soc. Trans.* **2007**, *35*, 910−911.

DOI: 10.1021/acsami.6b07628
ACS Appl. Mater. Interfaces 2016, 8, 28448−28457